

## Switching manifold approach to chaos synchronization

Jin-Qing Fang

*China Institute of Atomic Energy, P.O. Box 275-27, Beijing 102413, People's Republic of China*

Yiguang Hong

*Institute of Systems Science, Academia Sinica, Beijing 100080, People's Republic of China*

Guanrong Chen

*Department of Electrical and Computer Engineering, University of Houston, Houston, Texas 77204-4793*

(Received 26 June 1998)

In this Rapid Communication, a switching manifold approach is proposed for synchronizing chaos. The effectiveness of this nonlinear control strategy is demonstrated by both theoretical analysis and numerical simulations on two typical chaotic systems: the Lorenz and the modified Lorenz systems.

[S1063-651X(99)51603-6]

PACS number(s): 05.45.-a, 89.70.+c, 43.72.+q

### I. INTRODUCTION

The problems of controlling and synchronizing chaos can be formulated under a unified framework [1]. These two subjects have been intensively studied in the last decade [1,2]. Chaos synchronization has many potential applications in laser physics, chemical reactor, secure communication, biomedical science, and so on [3].

It is known that linear or linearized control methods are not always possible for controlling nonlinear systems, and nonlinear control methods prove to be often necessary, especially for chaotic systems [3,4]. Some nonlinear control techniques have even been extended to synchronization of hyperchaos and spatiotemporal chaos [4,5]. One typical method is the variable structure (or sliding mode) control, which has some successful applications for chaotic systems [6].

In this Rapid Communication, we further extend our method [6] to performing synchronization of two chaotic systems with different initial conditions. In addition to theoretical analysis, two Lorenz systems and two modified Lorenz systems are simulated to demonstrate the effectiveness of this method.

Consider two  $n$ -dimensional chaotic systems,

$$\dot{x} = F(x), \quad x \in R^n, \quad (1)$$

$$\dot{y} = F(y) + G(x)u, \quad y \in R^n, \quad u \in R^m, \quad (2)$$

where  $F$  is a vector-valued nonlinear function satisfying some defining conditions, and  $G(x)$  is an  $n \times m$  matrix-valued nonlinear function to be determined along with the controller  $u = u(x, y)$ .

The goal here is to force the two coupled systems to be synchronized even if they have different initial conditions. As usual, we call system (1) the master system, and system (2), the slave system.

The basic controller design principle is outlined as follows. To start with, a switching manifold containing the desired chaotic target (for synchronization) of the master system, is found. Then, using a nonlinear control strategy, the

state of the slave system is driven to move toward the manifold from any nearby place. In much the same way, another switching manifold is obtained for a chaotic state nearby the target, and the trajectory is forced to slide onto it. The control law so designed can be in a very simple nonlinear form. The effectiveness of such a control strategy can be analyzed by both theoretical analysis and numerical simulation, as demonstrated below.

### II. ANALYSIS OF SWITCHING MANIFOLDS

To illustrate the proposed control method and design procedure, it is especially convenient to use examples. The well-known Lorenz system and its modified version [7] are taken as examples for this purpose.

Example 1. Consider two coupled Lorenz systems, where the first system is given by

$$\begin{aligned} \dot{x}_1 &= -\sigma(x_1 - x_2) \\ \dot{x}_2 &= \rho x_1 - x_2 - x_1 x_3 \\ \dot{x}_3 &= x_1 x_2 - b x_3, \end{aligned} \quad (3)$$

and the second one has the same form, with  $x_i$  being replaced by  $y_i, i = 1, 2, 3$ , respectively, which are assumed to have two sets of different initial conditions.

Example 2. Consider two coupled modified Lorenz systems [7], in which the two product terms  $x_1 x_3$  and  $x_1 x_2$  in Eq. (3) are replaced by  $20x_1 x_3$  and  $5x_1 x_2$ , respectively, with two different initial conditions.

To simplify our presentation, we only analyze Example 1 here. By adding a controller into the right-hand side of the first equation of the slave system, we have

$$\dot{y}_1 = -\sigma(y_1 - y_2) + u. \quad (4)$$

Then, by subtracting Eq. (3) from the slave system, with the first equation being replaced by Eq. (4), and by defining the synchronization error as

$$e_i = y_i - x_i, \quad i = 1, 2, 3,$$

we obtain the synchronization error dynamics,

$$\begin{aligned} \dot{e}_1 &= -\sigma(e_1 - e_2) + u \\ \dot{e}_2 &= \rho e_1 - e_2 - e_1(x_3 + e_3) - e_3 x_1 \\ \dot{e}_3 &= e_1(x_2 + e_2) + x_1 e_2 - b e_3, \end{aligned} \quad (5)$$

where, compared with Eq. (2),  $G = (1, 0, 0)^T$ . Moreover, let the controller be

$$u = u_{eq} + u_0, \quad |u_0| \leq \epsilon, \quad (6)$$

where  $u_{eq}$  and  $u_0$  are to be determined, and  $\epsilon > 0$  is the allowable bound for the control inputs.

For synchronization purpose, as mentioned above, the first step is to find a suitable switching manifold, and then to design an effective nonlinear control to drive the error state to move toward this stable manifold. In so doing, the error state will eventually approach zero along (or near) the manifold. Select the manifold to be in the form

$$s = s(e), \quad (7)$$

which has to be specified such that (i) it contains the target,  $e = 0$ , and (ii)  $\partial s / \partial u \neq 0$  almost everywhere (near  $e = 0$ ).

For the error dynamical system (5), the desired manifold (usually not unique) can be taken as

$$s(e) = b e_3 - e_1^2 = 0, \quad (8)$$

where  $b$  is a positive constant. For this chosen manifold, it is easy to verify that the two conditions, (i) and (ii) described above, can be satisfied: first,  $e = 0$  is contained in the manifold; second, the vector  $G = (1, 0, 0)^T$  is transversal to the manifold at the point  $e = 0$ . This is because

$$\dot{s} = b[e_1(x_2 + e_2) + x_1 e_2 - b e_3] - 2e_1[-\sigma(e_1 - e_2) + u], \quad (9)$$

which implies

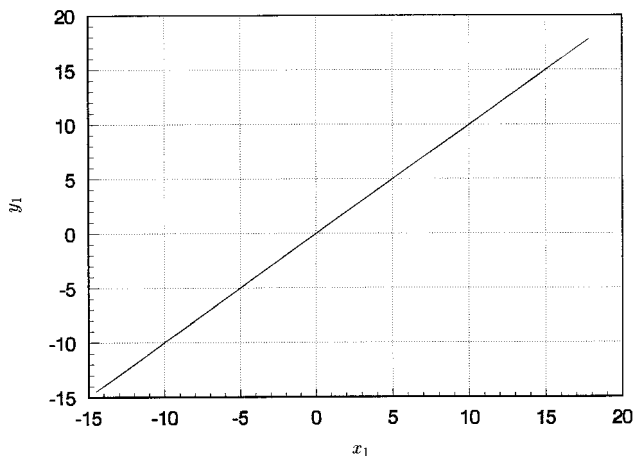


FIG. 1. Synchronization between  $y_1$  and  $x_1$  after a transient (2000 steps) for Example 1 with different initial conditions controlled by the controller (13) with  $u_{eq} \neq 0$ .

$$\partial \dot{s} / \partial u = -2e_1, \quad (10)$$

and this does not vanish along manifold (8) except when  $e_1 = 0$ . Therefore, when  $e_1 \neq 0$ ,  $\dot{s}$  can be directly controlled by  $u$ .

Next, we study the dynamical behavior of the error system (5) when it is confined on the manifold by the controller  $u$ .

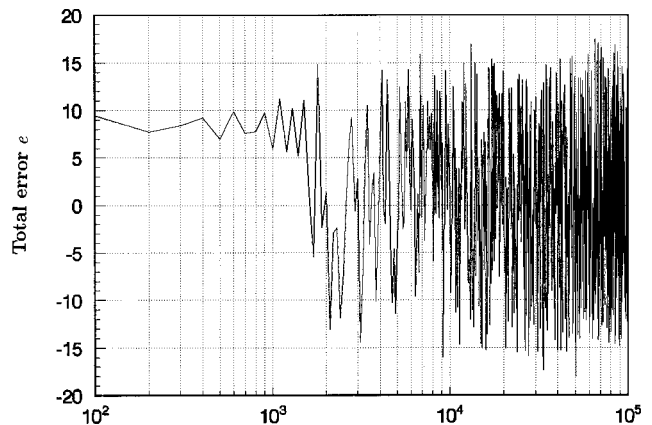
Remark 1. If  $G$  is taken as  $(0, 1, 0)^T$ , then the controlled Lorenz system becomes

$$\begin{aligned} \dot{e}_1 &= -\sigma(e_1 - e_2) \\ \dot{e}_2 &= \rho e_1 - e_2 - e_1(x_3 + e_3) - e_3 x_1 + u \\ \dot{e}_3 &= e_1(x_2 + e_2) + x_1 e_2 - b e_3. \end{aligned} \quad (11)$$

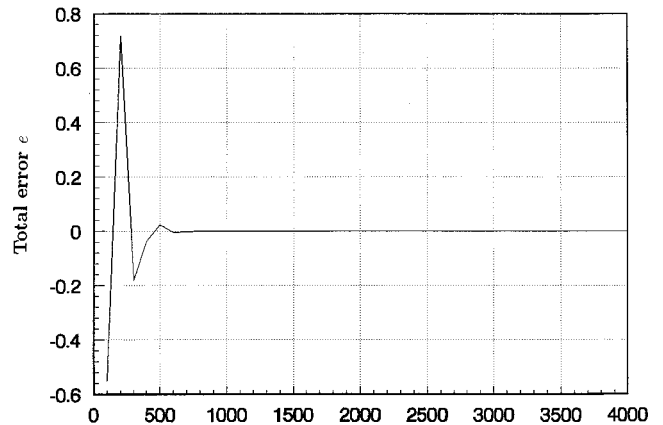
In this case, a switching manifold can be selected as

$$s(x) = b e_3 - e_2^2 = 0. \quad (12)$$

The manifolds (8) and (12) can be used simultaneously for the two examples studied in this paper, as shown below by numerical simulations.



(a) Number of time steps T



(b) Number of time steps T

FIG. 2. Total dynamical error  $e = \sum_{i=1}^3 e_i$  for Example 1 with different initial conditions controlled by the same controller (13), as in Fig. 1. In this figure, (a)  $u_{eq} = 0$ ; (b)  $u_{eq} \neq 0$ . (All of ordinate is dimensionless.)

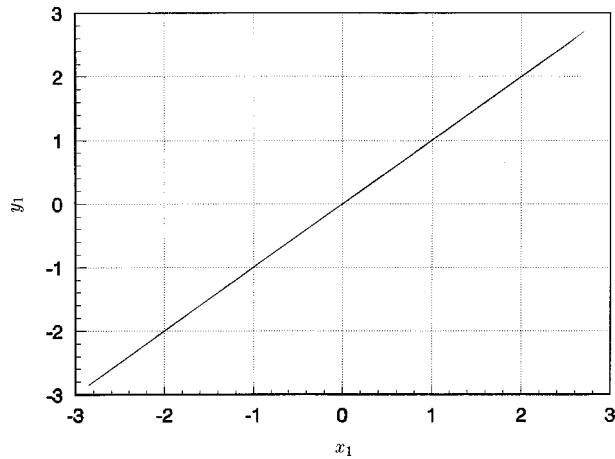


FIG. 3. Synchronization between  $y_1$  and  $x_1$  after a transient (2000 steps) for Example 2 with different initial conditions controlled by the controller (13) with  $u_{eq} \neq 0$ . (Ordinate is dimensionless.)

### III. CONTROLLER DESIGN PROCEDURE

Recall that the task of control is to force  $s$  in Eq. (9) to tend to zero. Therefore, the controller design must follow this principle: to drive all the error states, typically those nearby the manifold, to converge onto the stable manifold.

Consider Eq. (9) again. If all the variables  $e_1, e_2, e_3$  can be directly measured, then the control law can be chosen in the form of Eq. (6), in which  $u_{eq}$  is designed to ensure  $\dot{s} = 0$  whenever  $s = 0$ . Intuitively,  $u_{eq}$  plays the dominant control, whenever  $u_0$  fails to achieve synchronization alone. Observe that  $-b^2 e_3 = -bs - be_1^2$ , so that Eq. (9) can be rewritten as

$$\dot{s} = b[e_1(x_2 + e_2) + x_1 e_2] - bs - be_1^2 + 2\sigma e_1(e_1 - e_2) - 2e_1 u.$$

Based on this, it is easy to see that we can use

$$u_{eq} = (\sigma - b/2)(e_1 - e_2)$$

and

$$u_0 = \epsilon \operatorname{sgn}[e_1 s];$$

that is,

$$u = (\sigma - b/2)(e_1 - e_2) + \epsilon \operatorname{sgn}[e_1(b e_3 - e_1^2)]. \quad (13)$$

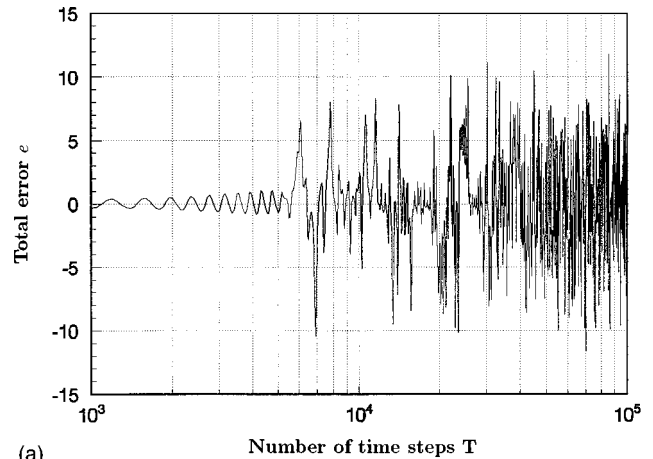
To this end, the controlled system (9) with controller (13) becomes

$$\dot{s} = -bs - \epsilon \operatorname{sgn}[e_1 s] + d(t), \quad (14)$$

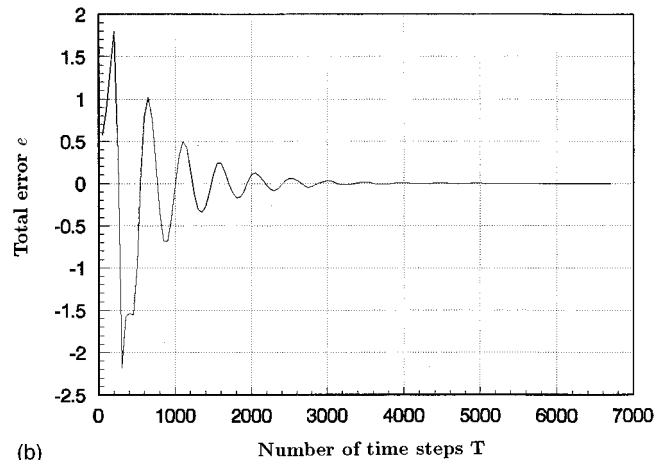
where  $d = b(e_1 x_2 + x_1 e_2)$  may be viewed as a disturbance. Because this type of controller is robust, such disturbance can be attenuated, as well documented in the conventional nonlinear control literature.

Remark 2. Even if  $\epsilon = 0$  is used in the control law, namely,

$$u = u_{eq} = (\sigma - b/2)(e_1 - e_2), \quad (15)$$



(a)



(b)

FIG. 4. Total dynamical error  $e = \sum_{i=1}^3 e_i$  for Example 2 with different initial conditions controlled by the same controller (13), as in Fig. 3. In this figure, (a)  $u_{eq} = 0$ ; (b)  $u_{eq} \neq 0$ . (All of ordinate is dimensionless.)

synchronization is still possible. In this case, however, the robustness enhanced by the additional control term  $u_0$  is generally lost. With a suitable  $\epsilon > 0$ , the convergence rate can be significantly improved.

Remark 3. If system (11) is considered along with the manifold (12), the following control law works as well:

$$u = u_{eq} + \epsilon \operatorname{sgn}[e_2(b e_3 - e_2^2)], \quad (16)$$

$$u_{eq} = e_1[e_3 - (\rho - b/2)] + (1 - b/2)e_2. \quad (17)$$

This is similar to the controllers (13) and (15).

Remark 4. If  $u_{eq} = 0$  is used in the controller, then the above control task fails, at least in our simulations.

Remark 5. If only a simple linear feedback,  $u = -k e_i, k > 0, i = 1$  or  $3$ , is used, the above control task also fails in our simulations.

### IV. SIMULATION AND DISCUSSION

The Lorenz system has a familiar chaotic attractor for the parameters set  $\sigma = 10$ ,  $b = 8/3$ , and  $\rho = 28$ , whereas the modified Lorenz system has a chaotic attractor for  $\sigma = 16$ ,  $b = 4$ , and  $\rho = 45.92$ .

To demonstrate the effectiveness of the developed control method, we have studied various numerical simulations for synchronization between two identical Lorenz systems (see Examples 1 and 2) with different initial conditions.

Figure 1 shows the dynamical behavior of the synchronization between  $y_1$  and  $x_1$  after a transient (2000 steps) for Example 1 with different initial conditions:  $x(0) = (0, -1, 0)^T$  and  $y(0) = (0.05, -0.05, 0.01)^T$ . The controller is given by Eq. (13), namely,

$$u = u_{eq} + u_0 = (\sigma - b/2)(e_1 - e_2) + \epsilon \operatorname{sgn}[e_1(b e_3 - e_1^2)].$$

Figure 2 shows the total dynamical error  $e = \sum_{i=1}^3 e_i$ , associated with Fig. 1. In Fig. 2(a),  $u_{eq} = 0$ ; in 2(b),  $u_{eq} \neq 0$ .

Figure 3 shows the synchronization behavior between  $y_1$  and  $x_1$  after a transient (2000 steps) for Example 2 with different initial conditions:  $x(0) = (0.01, -0.01, 0.05)^T$  and  $y(0) = (0.05, -0.05, 0.01)^T$ . The controller is also given by Eq. (13).

Figure 4 shows the total dynamical error  $e = \sum_{i=1}^3 e_i$ , associated with Figure 3. In Fig. 4(a),  $u_{eq} = 0$ ; in 4(b),  $u_{eq} = 0$ . Simulation results using controller (16) for Examples 1 and 2 are very similar to Fig. 4.

It is clear from Figs. 1–4 that these numerical simulations indeed have verified that the above theoretical analysis is correct and our nonlinear control strategy is effective. More specifically, using either controller (13) or (16), precise synchronization is achieved for the two examples. However, the control fails for synchronizing these two coupled systems, as shown in Figs. 2(b) and 4(b), if  $u_{eq} = 0$  is taken in Eq. (13) or (16). The control also fails if only a simple linear feedback  $u = k e_i$  ( $i = 1$  or  $3$ ) is used. This demonstrates the advantage of the proposed control strategy. The main idea and the method of this Rapid Communication can be extended to other chaotic/hyperchaotic systems in principle.

#### ACKNOWLEDGMENTS

This work was supported by the NNSFC, NCPC, and NNISFC.

- 
- [1] C. W. Wu, T. Yang, and L. O. Chua, *Int. J. Bifurcation Chaos Appl. Sci. Eng.* **6**, 455 (1996); M. di Bernardo, *ibid.* **6**, 557 (1996); J.-Q. Fang and M. K. Ali, *Discrete Dyn. Nature Soc.* **1**, 283 (1997).
- [2] H. G. Winful and L. Rahman, *Phys. Rev. Lett.* **65**, 1575 (1990); D. W. Peterman, N. Ye, and P. E. Wigen, *ibid.* **74**, 1740 (1995).
- [3] G. Chen and X. Dong, *From Chaos to Order: Methodologies, Perspectives and Applications* (World Scientific, Singapore, 1998).
- [4] V. Petrov and K. Showalter, *Phys. Rev. Lett.* **76**, 3312 (1996); H. Nijmeijer and A. J. van der Schaft, *Nonlinear Dynamical Control Systems* (Springer-Verlag, New York, 1991).
- [5] J.-Q. Fang, *Prog. Phys.* **16**, 1 (1996) (in Chinese); **16**, 137 (1996); M. K. Ali and J.-Q. Fang, *Phys. Rev. E* **55**, 5285 (1997); *Discrete Dyn. Nature. Soc.* **1**, 179 (1997). J.-Q. Fang and M. K. Ali, *Chin. Phys. Lett.* **4**, 823 (1997); *Nucl. Sci. Technol.* **1**, 129 (1997); **8**, 193 (1997).
- [6] X. Yu, *Int. J. Syst. Sci.* **27**, 355 (1997); T.-L. Liao and N.-S. Huang, *Phys. Lett. A* **29**, 262 (1997); J.-Q. Fang, Y. G. Hong, H. S. Qin, and G. Chen (unpublished).
- [7] K. M. Cuomo and A. V. Oppenheim, *Phys. Rev. Lett.* **71**, 65 (1993).